1994

Intergranular and intragranular critical currents in silver-sheathed Pb-Bi-Sr-Ca-Cu-O tapes

K. Muller
CSIRO, Australia

C. Andrikidis
CSIRO, Australia

Hua-Kun Liu
University of Wollongong, hua@uow.edu.au

S. X. Dou
University of Wollongong, shi@uow.edu.au

Intergranular and intragranular critical currents in silver-sheathed Pb-Bi-Sr-Ca-Cu-O tapes

K.-H. Müller and C. Andrikidis
Commonwealth Scientific and Industrial Research Organization, Division of Applied Physics, Lindfield, Australia 2070

H. K. Liu and S. X. Dou
Centre for Superconducting and Electronic Materials, University of Wollongong, Australia 2522
(Received 13 April 1994)

The role of the intergranular and intragranular critical current densities in silver-sheathed Pb-Bi-Sr-Ca-Cu-O tapes is investigated by means of magnetic-moment measurements in perpendicular field at different temperatures using a superconducting quantum interference device magnetometer. We find that low-field magnetic-moment loops are mainly caused by the intergranular (transport) critical current density J_c^J but that in high fields the contribution from the intragranular critical current density J_c^G becomes significant. The low-field data can be described well in terms of a critical-state model for a thin strip of a homogeneous type-II superconductor in a perpendicular field where J_c^J flows over the entire tape. The high-field data require in addition a description in terms of a critical-state model for the grains where J_c^G circulates in each grain. Strong mechanical bending of the tape causes J_c^J to disappear while J_c^G is unaffected. The experimental data reveal the hysteretic nature of J_c^J which is caused by the trapping of flux in grains. In all the tapes measured, J_c^J is found to be much smaller than J_c^G. Comparing the remanent J_c^J with J_c^G in different tapes, we find that strong pinning in grains does not imply a high remanent intergranular critical current density.

I. INTRODUCTION

Shortly after the discovery of the high-temperature superconductors it was noticed that the intergranular (transport) critical current density J_c^J in polycrystalline samples is limited by the weak-link behavior of the grain boundaries.[1] This deleterious influence of grain boundaries is believed to be due to the shortness of the coherence length ξ in these cuprate oxides, which is much smaller than the coherence length in conventional superconductors.[2] Initially some magnetic data were misinterpreted and the very large intragranular critical current density J_c^G inside grains, which produces a strong magnetic signal in high fields, was incorrectly associated with J_c^J. Later, experiments on bicrystal grain boundaries have demonstrated that a current across a grain boundary in the highly anisotropic cuprate oxides decreases very rapidly with increasing grain misorientation[3] and thus the random orientation of the grains is blamed for the low J_c^J in polycrystalline samples.

In contrast, a very high intergranular critical current density J_c^J is achieved for Ag-sheathed $(Pb,Bi)_2Sr_2Ca_2Cu_3O_{10+y}$ tapes[4-7] (PBSCCO tapes), which are extremely promising for applications. The high J_c^J in these tapes seems to be caused by the strong alignment of the grains which is achieved by pressing and rolling of the PBSCCO powder encapsulated in a silver sheath. The finished tape microstructure then consists of small platelets with large aspect ratios of typically less than 1 μm thickness in the c direction and 20 μm diameter in the a and b directions. The platelets generally align within 5°–10° with the c direction perpendicular to the plane of the tape and the a or b directions oriented at random from platelet to platelet. At least two types of grain boundaries exist in these tapes, c-oriented grain boundaries and a- or b-oriented ones.[8]

So far little is known about the interplay between intergranular and intragranular critical current densities, J_c^J and J_c^G, respectively, and how essential a high J_c^G is to obtain a high J_c^J.[8] Caplin *et al.*[9] recently compared the magnetization of a tape with that of the powder scraped out of the tape. They found that in their tape $J_c^G \simeq 10 \times J_c^J$ and they argued that the limiting factor for J_c^J is J_c^G itself.

In this paper we demonstrate that the intergranular and intragranular critical current densities J_c^J and J_c^G for approximately zero applied field can be determined quantitatively from measurements of the tape's remanent magnetic moment m_R as a function of the maximum applied magnetic field H_m. The reason for J_c^J and J_c^G not being determined previously by others from magnetic measurements on tapes seems to be the lack of knowledge of how to calculate the magnetic moment of a type-II superconductor in the shape of a flat tape in a perpendicular magnetic field. Such calculations have only been done very recently.[10,11]

In Sec. II we briefly describe the experiment to measure the magnetic moment m as a function of the magnetic field, applied perpendicular to the tape. In Sec. III we discuss the equations which describe the magnetic moment m of a flat strip (tape) of a granular type-II superconductor in a perpendicular applied field. Intergranular and intragranular contributions are evaluated in certain field limits which allow the determination of J_c^J and J_c^G from the $m_R(H_m)$ data.

In Sec. IV we discuss the results and obtain the ratio between J_c^J and J_c^G and how J_c^J and J_c^G depend on temperature. We give clear evidence for the existence of both

intergranular and intragranular contributions by measuring the remanent magnetic moment versus H_m after bending and straightening of the tape, which causes J_c^J to diminish. We also show that the magnetic moment reveals the hysteretic nature of J_c^J. Finally in Sec. V we summarize our findings.

II. EXPERIMENT

The magnetic moments m of three different silver-sheathed single-filament PBSCCO (2223) tapes (1, 2, and 3) were measured as a function of the magnetic field H_a applied perpendicular to the tape surface, using a commercial Quantum Design superconducting quantum interference device (SQUID) magnetometer. A 5-cm scan was used and the field was swept in the no-overshoot mode. Hysteretic measurements were made for fields between ± 5 T at temperatures of 5–77 K. Remanent magnetic-moment measurements where the maximum field was varied from 1 mT to 5 T required about 8 h each. The tapes were prepared employing the powder-in-tube method. The details concerning this method have been reported in Ref. 12. X-ray diffraction indicated that the core of the tapes consisted of almost pure 2223 phase with only very small amounts of 2212 phase present. The transport (intergranular) critical current densities of tapes 1 and 3 were measured at 77 K electrically using the four-point probe method and found to be 4500 and 16 000 A cm^{-2}, respectively.

III. THEORETICAL MODEL

The magnetic moment $\mathbf{m}$ is defined as

$$\mathbf{m}=\tfrac{1}{2}\int \mathbf{r}\times\mathbf{J}(\mathbf{r})d^3r \ , \tag{1}$$

where $\mathbf{r}$ is the space vector and $\mathbf{J}$ the local current density. In the case of a PBSCCO tape where the magnetic field is applied perpendicular to the tape surface (parallel to the c direction of the grain platelets), the component m of $\mathbf{m}$, in the direction of the applied field, can be split into an intergranular and an intragranular part,[13]

$$m=m^J+\sum_i m_i^G \ . \tag{2}$$

Here m^J is the magnetic moment originating from the intergranular current which flows along the whole length of the tape. Because the intergranular current is related to the grain-boundary Josephson junction currents the superscript J is used in m^J. The second term in Eq. (2) represents the sum over all the magnetic moments of the grains and thus the superscript G is used in $\sum_i m_i^G$. While m^J is determined by the intergranular critical current density J_c^J (often also referred to as the transport critical current density), $\sum_i m_i^G$ is determined by the intragranular critical density J_c^G (assuming here that all grains have the same J_c^G). The value of J_c^G is determined by the pinning of flux lines in the grains. Figure 1 shows schematically the intergranular and intragranular current densities.

Recently Brandt and Indenbom[10] as well as Zeldov *et al.*[11] have derived analytical expressions for the magnetic moment of a thin strip (or tape) of a homogeneous (nongranular) type-II superconductor in a perpendicular applied magnetic field. Employing a procedure proposed earlier by Norris,[14] they showed that it is possible to use conformal mapping and the method of images to obtain the current density in the central region of the strip where the current density $|J|$ is less than the critical current density J_c. This is in contrast to a slab in parallel field where only regions with $J=J_c$ and $J=0$ exist.

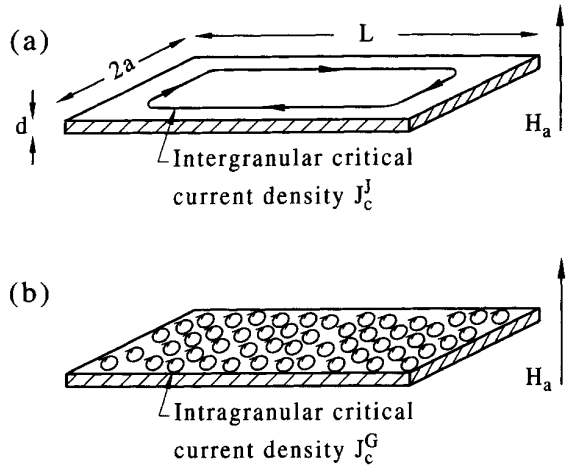

FIG. 1. Schematic of intergranular and intragranular currents in a superconducting single-filamentary PBSCCO tape induced by a perpendicular applied magnetic field.

In the following, the length of the superconducting strip is L, its half-width a, and the strip thickness d. Assuming that the critical current density J_c is independent of the local induction $\mathbf{B}(\mathbf{r})$ with $B\simeq\mu_0 H$ and that, furthermore, $d\ll a$, the following analytical expressions can be derived for the intergranular magnetic moment m^J.[10]

(i) For the virgin intergranular magnetic moment m_V^J one obtains

$$m_V^J=-\pi a^2 L H_c \tanh(H_a/H_c) \ , \tag{3}$$

where H_a is the applied field and

$$H_c=J_c^J d/\pi \ . \tag{4}$$

(ii) For the upper ($\uparrow$) and lower ($\downarrow$) branches of the intergranular magnetic moment $m_{\uparrow\downarrow}^J$ one obtains

$$m_{\uparrow\downarrow}^J=\mp\pi a^2 L H_c\{\tanh(H_m/H_c)+2\tanh[(\pm H_a-H_m)/2H_c]\} \ , \tag{5}$$

where H_m is the maximum applied field H_a.

In addition, from Eqs. (3) and (5) one finds

$$\left.\frac{\partial m_V^J}{\partial H_a}\right|_{H_a=0}=\left.\frac{\partial m_\uparrow^J}{\partial H_a}\right|_{H_a=H_m}=-\pi a^2 L \ . \tag{6}$$

This is an important result because it states that the slope of the virgin intergranular magnetic moment at zero field and the slope of the upper branch of the intergranular magnetic moment at $H_a=H_m$ are independent of J_c^J and only depend on the superconducting strip length L and

half-width a. A similar expression for the slopes of m_V^J and $m_\uparrow^J$ has been derived by Angadi *et al.*[15] for a disk-shaped superconductor in a perpendicular field.

For the remanent intergranular magnetic moment m_R^J one derives from Eq. (5)

$$m_R^J = -\pi a^2 L H_c[\tanh(H_m/H_c) - 2\tanh(H_m/H_c)] . \quad (7)$$

For $H_m \gg H_c$ one finds

$$m_R^J(H_m \to \infty) = \pi a^2 L H_c = d a^2 L J_c^J . \quad (8)$$

Thus the saturated intergranular magnetic moment is determined by the dimensions of the superconducting strip and the intergranular critical current density J_c^J.

The assumption of a J_c^J that is independent of the local magnetic field, used to derive the above expressions, is valid if $J_c^J(H)$ varies only insignificantly over a field interval of size H_c [Eq. (4)]. Fortunately in PBSCCO tapes (see Sec. IV) the characteristic field H_c has a rather small value and experimental data of the transport current show no significant drop over such a small magnetic field interval, making the assumption of a J_c^J that is independent of the local magnetic field a reasonable one.

So far we have given expressions for the intergranular magnetic moment m^J of the tape. The second part of the total magnetic moment m in Eq. (2), the intragranular magnetic moment $\sum_i m_i^G$, which originates from circulating currents in the grains, is difficult to derive over the full applied-field range. The reason is that it is not well known how the magnetic field meanders between grains and how to treat the demagnetizing effect in a complicated grain microstructure.[16,17] Despite this, $\sum_i m_i^G$ can be calculated in weak applied fields or at $H_a = 0$ after a very large field H_m has been applied.

In the case of a weak applied field such that $H(\mathbf{r})$ is less than the lower critical field of the grains, H_{c1G}, everywhere in the tape, only Meissner shielding currents are induced in the grains and

$$\left[\sum_i m_i^G\right]_{\text{Meissner}} \simeq -\frac{f_s}{1-n} 2aLdH_a , \quad (9)$$

where f_s is the volume fraction of superconducting grains and n the effective demagnetizing factor of the grains.

In the case where one reduces a very large applied magnetic field to zero, the intragranular current density J_c^G is still circulating in the grain platelets of radius R_G and the remanent intragranular magnetic moment becomes

$$\left[\sum_i m_i^G\right]_R (H_m \to \infty) = \tfrac{2}{3} aLdR_G J_c^G . \quad (10)$$

IV. RESULTS AND DISCUSSION

Figure 2 shows the experimental and calculated loops of the magnetic moment m of the Pb-Bi-Sr-Ca-Cu-O (2223) tape 1 at a temperature of $T = 5$ K in low fields up to $\mu_0 H_m = 22$ mT. The full curves represent the calculated total magnetic moment m. For the calculation Eqs. (3) and (5) for m^J and Eq. (9) for $\sum_i m_i^G$ were used. When

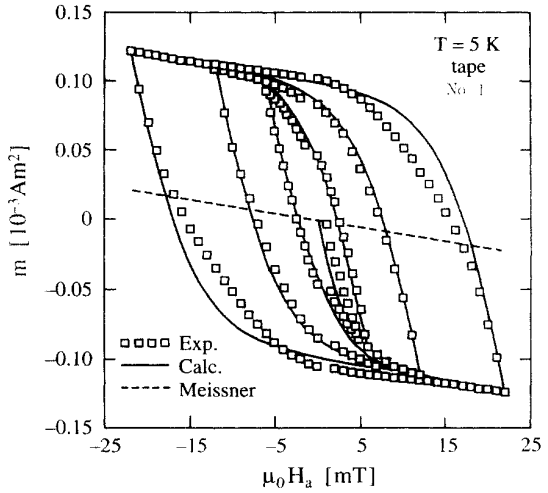

FIG. 2. Low-field magnetic-moment loops of tape 1 for $\mu_0 H_m = 6$, 12, and 22 mT at a temperature of 5 K. The full curves are theoretical results using Eqs. (3) and (5) for m^J. The dashed line shows the Meissner magnetic moment of the grains.

calculating m^J it was assumed that J_c^J is independent of H_m which, as will be shown below, is only correct for low H_m. Because the cross section of the superconducting filament is tapered at the ends and is more elliptical than rectangular, the values used for a and d correspond to those of a rectangle approximating the tape cross section. The dimensions of the tape 1 are $d = 35$ μm, $a = 1.35$ mm, and length $L = 5.9$ mm.

The dashed line in Fig. 2 indicates the Meissner magnetic moment of the grains [Eq. (9)] which causes the moment loops to tilt. The factor $f_s/(1-n)$ in Eq. (9) can be determined from this tilt. One finds $f_s/(1-n) \simeq 2.3$. Assuming that the volume fraction of superconducting grains is 0.9, the effective grain demagnetization factor is $n = 0.6$. Because the grain platelets shield each other,[16,17] the demagnetizing effect is less pronounced than one would expect for a single-grain platelet of 10 μm radius and 1 μm thickness in a perpendicular magnetic field where n is close to 1. The best fit to the experimental data at 5 K was obtained with $J_c^J = 2.8 \times 10^8$ A m^{-2}, which gives $\mu_0 H_c = 3.7$ mT [Eq. (4)]. It is important to notice that, due to the strong demagnetizing effect of the flat tape in a perpendicular field, a rather weak applied field of only about 5 mT already causes saturation of the intergranular magnetic moment m^J. The slope of m_V^J at $H_a = 0$ and $m_\uparrow^J$ at $H_a = H_m$ is given by Eq. (6) and the calculated value agrees well with the experimental one.

Figure 3 shows the experimental data of the total magnetic moment of tape 1 at 5 K in high fields of $\mu_0 H_m = 1$ and 5 T. The vertical line at $H_a \simeq 0$ represents the low-field loops of Fig. 2. The high-field loops consist of both intergranular and intragranular magnetic moments and a distinction between both cannot be made here, in contrast to the low-field loops where m is essentially m^J. The features in Fig. 3 are characteristic of loops which can be modeled using a critical-state model for grains, which takes the equilibrium magnetization of grains into

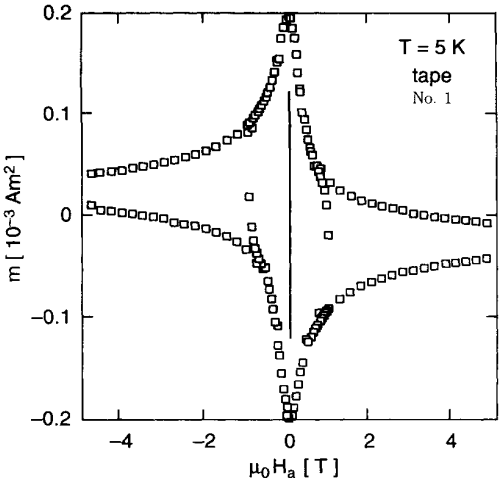

FIG. 3. High-field magnetic-moment loops of tape 1 for $\mu_0 H_m = 1$ and 5 T at a temperature of 5 K. Both m^J and $\sum m_i^G$ contribute to the total magnetic moment m. The vertical line at $H_a \simeq 0$ represents the low-field loops of Fig. 2.

account and where the intragranular J_c^G decreases with increasing magnetic field,[18] though a significant part of m will be due to the intergranular m^J.

Figure 4 shows the measured and calculated total remanent magnetic moment m_R of tap 1 as a function of the logarithm (base 10) of $\mu_0 H_m$ at three different temperatures. The characteristic features of the data are a shoulder (or the indication of a plateau) at low fields and saturation at high fields. The full curves in Fig. 4 represent the calculated intergranular m_R^J using Eq. (7)

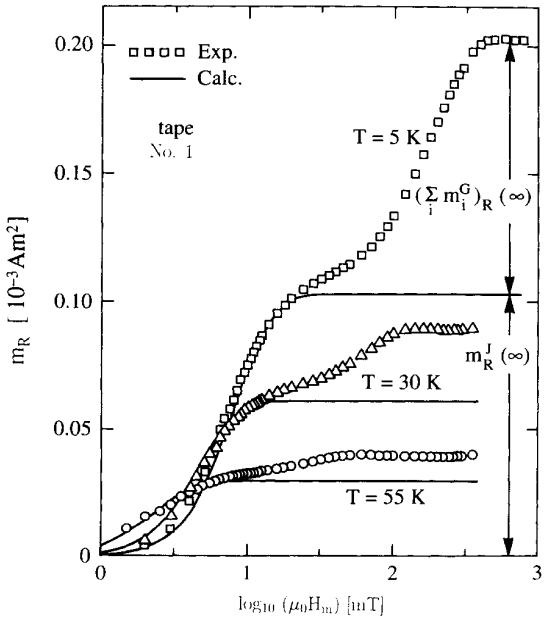

FIG. 4. Remanent magnetic moment m_R of tape 1 as a function of the maximum applied magnetic field H_m at different temperatures. The full curves show the theoretical results using Eq. (7). J_c^J and J_c^G can be obtained from this measurement.

where the same values for d, a, L, and $J_c^J(5\text{ K})$ as above in Fig. 2 were used. The calculations show that the shoulder is caused by the intergranular current which flows over the entire tape, where the position of the shoulder is at $H_m \simeq 4H_c$. The quantity $m_R^J(H_m \to \infty)$ given in Eq. (8) is indicated in Fig. 4. At high applied magnetic fields, flux penetrates the grains and the induced grain pinning current J_c^G contributes significantly to m_R. The intragranular magnetic moment $(\sum_i m_i^G)_R(H_m \to \infty)$ given by Eq. (10) is also indicated in Fig. 4, from which the intragranular critical current density can be extracted. Using a grain radius of $R_G = 10\ \mu$m, which is typical for our tapes, and assuming that J_c^J is independent of H_m, one finds $J_c^G(5\text{ K}) = 5.4 \times 10^{10}\ \text{A m}^{-2}$ and therefore $J_c^G(5\text{ K}) \simeq 200 \times J_c^J(5\text{ K})$ for tape 1.

From measurements of the remanent magnetization m_R, as presented in Fig. 4, the temperature dependences of J_c^J and J_c^G can be obtained assuming that J_c^J is independent of H_m. The result is shown in Fig. 5 where $J_c^J(T)/J_c^J(5\text{ K})$ and $J_c^G(T)/J_c^G(5\text{ K})$ are plotted versus temperature T. It can be seen that J_c^G decreases more rapidly with increasing temperature than J_c^J.

If one exposes the tape to bending strain, cracks develop in the superconducting material which disrupt the intergranular current density J_c^J.[19] For tape 2 the remanent magnetization was measured as a function of the maximum applied field H_m for different bending diameters. First the tape was measured in its original unbent form; then the tape was bent along its length to a diameter of $D = 10$ mm. After straightening the tape, m_R was measured. Afterwards the tape was bent again to the smaller diameter of $D = 1.25$ mm and m_R was again measured after straightening. It is assumed that bending and straightening of the silver-sheathed tape does not significantly reduce the c-axis alignment of the grain platelets. The experimental results of m_R versus the loga-

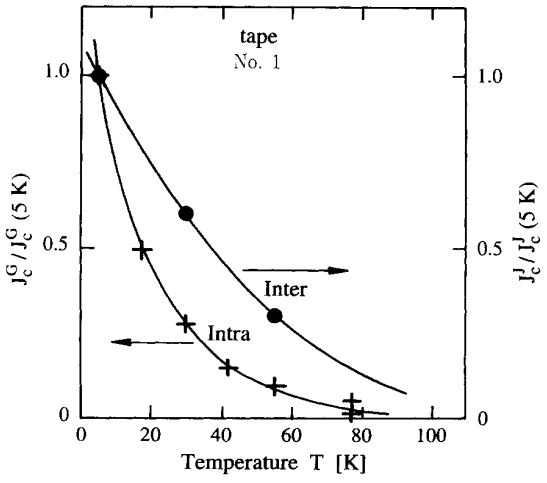

FIG. 5. Normalized intergranular critical current density J_c^J and intragranular critical current density J_c^G of tape 1 as a function of temperature obtained from measurements of the remanent magnetic moment $m_R(H_m)$ as shown in Fig. 4.

rithm (base 10) of $\mu_0 H_m$ are shown in Fig. 6. As can be seen, the intergranular part of m_R gradually disappears with increasing bending. For $D=10$ mm one finds that J_c^J is reduced by a factor of about 0.4. In the case of $D=1.25$ mm essentially only the intragranular part $(\sum_i m_i^G)_R$ of m_R remains, indicating that practically no current is flowing over the entire tape. The drop of J_c^J with increased bending is similar to that measured electrically for other tapes.[19] There still will be clusters of grains in the tape over which a considerable current is flowing even after very strong bending, but these clusters seem to be too small in size to contribute significantly to m_R. The field H_m at which $\sum_i m_i^G$ saturates is proportional to $J_c^G R_G$ and does not change with bending (Fig. 6), which indicates that bending does not cause grains to break and reduce the average grain size. The dashed curve in Fig. 6 shows the difference

$$[m_R(\text{no bend}) - m_R(D=1.25\text{ mm})]$$

which closely represents the actual intergranular magnetic moment m_R^J. As can be seen, the experimental m_R^J is different in shape at high fields from the calculated one shown in Fig. 4. In Fig. 4 all the calculated intergranular magnetic moments m_R^J increase initially and then stay constant while the experimental m_R^J in Fig. 6 (dashed line) drops at about 100 mT and stays constant in higher fields. The reason for this experimentally observed drop is the hysteretic behavior of the intergranular critical current density J_c^J in tapes caused by trapped magnetic flux in the grains. Electrical four-point probe measurements of J_c^J of tapes and polycrystalline samples have revealed a dependence of J_c^J on the magnetic-field history.[4,20–22] If after zero-field cooling one applies a field H_m and measures J_c^J after switching the field off, one finds that the remanent critical current density $J_{cR}^J \equiv J_c^J(H_a=0, H_m^{\downarrow})$ stays constant for $0 \le H_m \le H_{c1G}$, decreases in the range $H_{c1G} < H_m < 2R_G J_c^G$, and stays constant for $H_m > 2R_G J_c^G$ as shown schematically in Fig. 7. Explanations for the origin of the hysteretic behavior of J_c^J have been given by several authors.[20–23] The experimental data for m_R^J in Fig. 6 can be reproduced well using Eq. (7) if an H_m-dependent J_{cR}^J as shown in Fig. 7 is used for J_c^J in Eqs. (4) and (7). From the above discussion it becomes clear that from measurements of $m_R(H_m)$ the remanent critical current density J_{cR}^J and not $J_c^J(H_a=0)$ can be extracted. For a direct comparison of the magnetically measured J_c^J with the electrically measured one, corrections have to be made for the effect of flux creep. Because of the longer measuring time in the case of a magnetic measurement, the magnetically determined J_c^J is smaller than the electrically measured one.[24]

Taking the hysteretic nature of J_c^J into account, the above derived values for $J_c^G(T)$ of tape 1 (Fig. 4) represent an underestimation of about 20% at 5 K but the error is smaller at higher temperatures where the hysteretic behavior of J_c^J is less pronounced.[25] The error in J_c^G does not affect the basic finding presented in Fig. 5 where J_c^G drops more rapidly than J_c^J with increasing temperature.

Figure 8 shows the remanent magnetic moment m_R versus the logarithm (base 10) of the maximum applied field H_m for tape 3, which has the highest transport current density. For comparison the result of tape 2, previously shown in Fig. 6, is also displayed. Figure 8 also shows the remanent magnetization m_R after bending the tapes 2 and 3 to the small diameter $D=1.25$ mm followed by straightening. The dashed curves in Fig. 8 represent the actual intergranular magnetic moments m_R^J defined as

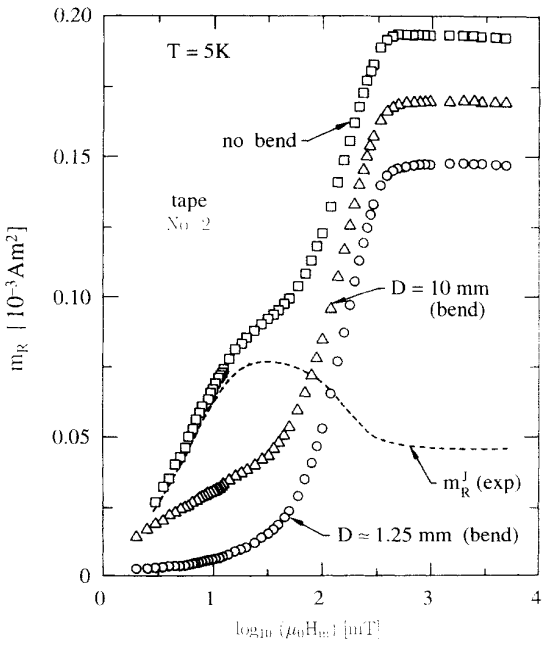

FIG. 6. Remanent magnetic moment of tape 2 versus the maximum applied field H_m for no bending of the tape, 10-mm bending diameter D, and 1.25-mm bending diameter. After each bending the tape was straightened and the magnetic moment measured. The dashed curve shows the experimental intergranular remanent magnetic moment m_R^J obtained by subtracting the "$D \simeq 1.25$ mm" data from the "no bend" data.

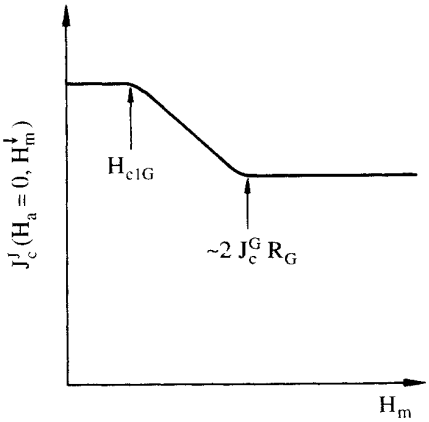

FIG. 7. Schematic drawing of the remanent intergranular critical current density $J_c^J(H_a=0, H_m^{\downarrow})$ versus the maximum field H_m. H_{c1G} is the lower critical field of the grains.

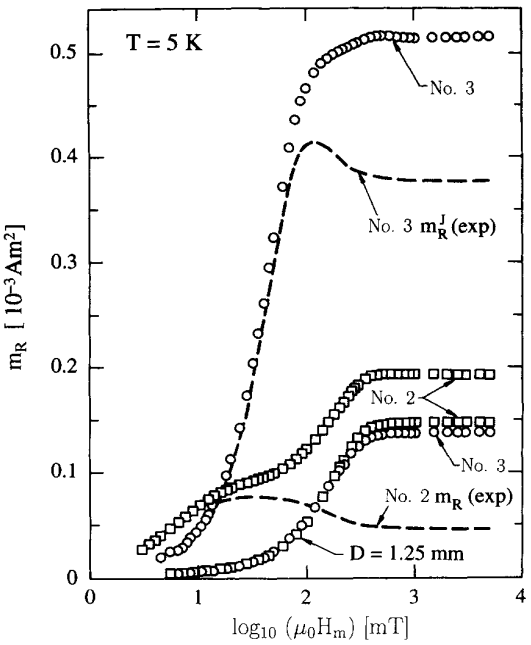

FIG. 8. Remanent magnetic moments of tapes 2 and 3 versus the maximum applied field H_m for no bending of the tapes and for "$D \simeq 1.25$ mm" bending. The dashed curves show the experimental intergranular magnetic moment m_R^J obtained by subtracting the "$D \simeq 1.25$ mm" data from the "no bend" data.

$$[m_R(\text{no bend}) - m_R(D = 1.25 \text{ mm})] .$$

The drop of the experimental m_R^J at about 100 mT is again due to the hysteretic nature of J_c^J. Taking the dimensions of tape 3 into account ($d = 60$ μm, $a = 1.3$ mm, $L = 5.8$ mm), one finds from Eq. (8) the value $J_c^J(5\text{ K}) \simeq 1 \times 10^9$ A m^{-2}. This is about 3.5 times larger than $J_c^J(5$ K) of tape 1. From the remanent magnetic moment for the bent tape 3 one estimates, using Eq. (10), $J_c^G \simeq 4.5 \times 10^{10}$ A m^{-2} and thus, for tape 3, $J_c^J(5\text{ K}) \simeq 45 \times J_c^G(5\text{ K})$.

The fact that J_c^G for both tapes 1 and 3 is about the same, though the intergranular critical current densities J_c^J are quite different, seems to indicate that a high intergranular critical current density $J_c^J(H_a = 0, H_m^{\downarrow},)$ does not require a high J_c^G in grains. Thus strong pinning of flux lines in grains seems not to be important to achieve a high $J_c^J(H_a = 0, H_m^{\downarrow})$. Instead, it appears that solely a high Josephson current density across grain boundaries is of importance, which can be achieved by a high degree of grain alignment and a tape fabrication procedure which ensures clean grain boundaries.

The relative magnitude between m_R^J and $(\sum_i m_i^G)_R$ (Figs. 4 and 8) indicates that dimensional scaling[26,27] (scaling of m with sample size) of the magnetic response in tapes can only be observed if J_c^J is very high. Otherwise, in low-J_c^J tapes, the non-negligible intragranular magnetic contribution causes nonscaling behavior.

V. CONCLUSIONS

In order to further improve the current-carrying capacity of silver-sheathed PBSCCO tapes, it is necessary to elucidate the role of both intergranular and intragranular critical current densities, J_c^J and J_c^G. At low fields the magnetic-moment loop of a PBSCCO tape is that of a flat strip of a homogeneous type-II superconductor in a perpendicular field where the intergranular critical current density J_c^J flows over the entire strip. At high fields the intragranular current density J_c^G, which is a measure of the pinning of magnetic-field lines in the grains, contributes significantly to the magnetic response which is most dominant in tapes with low J_c^J. The intergranular critical current density J_c^J reveals itself in the form of a foot or shoulder in the m_R versus H_m data. Strong bending of the tape severely reduces the intergranular current and the remanent magnetic moment of a bent and then straightened tape in high fields discloses the intragranular critical current density J_c^G. From measurement of m_R as a function of H_m the hysteretic intergranular critical current $J_c^J(H_a = 0, H_m^{\downarrow})$, or remanent J_{cR}^J, can be extracted. Our experimental data indicate that a high J_{cR}^J is not correlated to a high J_c^G. In all tapes measured we find that J_{cR}^J is much smaller than J_c^G and the current-carrying capacity of tapes seems to be limited not by the pinning of flux at defects in grains but merely by the weak-link behavior of the grain boundaries. The m_R data do not provide information about the field dependence of J_c^J and J_c^G.

ACKNOWLEDGMENTS

The authors would like to thank Y. C. Guo for placing tape No. 3 at their disposal.

[1]R. L. Peterson and J. W. Ekin, Phys. Rev. B **37**, 9848 (1988).
[2]G. Deutscher, Physica C **153–155**, 15 (1988).
[3]D. Dimos, P. Chaudhari, and J. Mannhart, Phys. Rev. B **41**, 4038 (1990).
[4]T. Hikata, M. Ueyama, H. Mukai, and K. Sato, Cryogenics **30**, 924 (1990).
[5]K. Sato, T. Hikata, H. Mukai, M. Ueyama, N. Shibuta, T. Kato, T. Masuda, M. Nagata, K. Iwata, and T. Misui, IEEE Trans. Magn. **MAG-27**, 1231 (1991).
[6]H. K. Liu, Y. C. Guo, S. X. Dou, S. M. Cassidy, L. F. Cohen, G. K. Perkins, A. D. Caplin, and N. Savvides, Physica C **213**, 95 (1993).
[7]B. Hensel, J.-C. Grivel, A. Jeremie, A. Perin, A. Pollini, and R. Flükiger, Physica C **205**, 329 (1993).
[8]L. N. Bulaevskii, L. L. Daemen, M. P. Maley, and J. Y. Coulter, Phys. Rev. B **48**, 13 798 (1993).
[9]A. D. Caplin, S. M. Cassidy, L. F. Cohen, M. N. Cuthbert, J. R. Laverty, G. K. Perkins, S. X. Dou, Y. C. Guo, H. K. Liu, F. Lu, H. J. Tao, and E. L. Wolf, Physica C **209**, 167 (1993).
[10]E. H. Brandt and M. Indenbom, Phys. Rev. B **48**, 12 893 (1993).
[11]F. Zeldov, J. R. Clem, M. McElfresh, and M. Darwin, Phys.

Rev. B **49**, 9802 (1994).
[12]H. K. Liu, Y. C. Guo, and S. X. Dou, Supercond. Sci. Technol. **5**, 591 (1992).
[13]J. R. Clem, Physica C **153-155**, 50 (1988).
[14]W. T. Norris, J. Phys. D **3**, 489 (1970).
[15]M. A. Angadi, A. D. Caplin, J. R. Laverty, and Z. X. Shen, Physica C **177**, 479 (1991).
[16]G. Waysand, Europhys. Lett. **5**, 73 (1988).
[17]M. L. Hodgdon, R. Navarro, and L. J. Campbell, Europhys. Lett. **16**, 677 (1991).
[18]C. Andrikidis, K.-H. Müller, N. Savvides, S. X. Dou, and H. K. Liu, Cryogenics **32**, 411 (1992).
[19]S. X. Dou, Y. C. Guo, J. Yau, and H. K. Liu, Supercond. Sci. Technol. **6**, 195 (1993).
[20]J. E. Evetts and B. A. Glowacki, Cryogenics **28**, 641 (1988).
[21]M. E. McHenry, M. P. Maley, and J. O. Willis, Phys. Rev. B **40**, 2666 (1989).
[22]K.-H. Müller and D. N. Matthews, Physica C **206**, 275 (1993).
[23]A. I. D'yachenko, Physica C **213**, 167 (1993).
[24]M. P. Maley, P. J. Kung, J. Y. Coulter, W. L. Carter, G. N. Riley, and M. E. McHenry, Phys. Rev. B **45**, 7566 (1992).
[25]C. Takahashi, M. Komatsu, Y. Yaegashi, M. Nagano, H. Takahashi, K. Hamada, and A. Nagata, IEEE Trans. Appl. Supercond. **3**, 957 (1993).
[26]M. E. McHenry, P. J. Kung, M. P. Maley, J. O. Willis, and J. Y. Coulter, IEEE Trans. Appl. Supercond. **3**, 1143 (1993).
[27]J. E. Tkaczyk, R. H. Arendt, M. F. Garbauskas, H. R. Hart, K. W. Lay, and F. E. Luborsky, Phys. Rev. B **45**, 12 506 (1992).